J_ID: Z3S Customer A_ID: JMRI23911 Cadmus Art: JMRI23911 Ed. Ref. No.: 11-0978.R1 Date: 5-October-12 Stage: Page: 1

Technical Note

Assessment of Intracranial Blood Flow Velocities Using a Computer Controlled Vasoactive Stimulus: A Comparison Between Phase Contrast Magnetic Resonance Angiography and Transcranial Doppler Ultrasonography

Jackie Leung, MASc,[1] Amir Behpour, MD,[1,2] Neil Sokol, XX,[2] Arun Mohanta, MD,[1] and Andrea Kassner, PhD[1,2]*

AQ1

Purpose: To compare measurements of blood flow velocity (BFV) and BFV changes in the middle cerebral arteries (MCA) acquired from phase contrast magnetic resonance angiography (PCMRA) and transcranial Doppler ultrasound (TCD) during controlled manipulation of end-tidal partial pressure of carbon dioxide ($P_{ET}CO_2$).

Materials and Methods: In vivo TCD and PCMRA velocity data from the M1 segment in the MCA of nine healthy adult volunteers were acquired during precise targeting of $P_{ET}CO_2$ induced by a computer-controlled gas delivery system. Doppler spectra and phase contrast data were processed into time-averaged peak-velocity (TAPV) values for comparison. Changes in velocity between baseline and hypercapnia were analyzed in terms of velocity-based cerebrovascular reactivity (CVR).

Results: Good correlation between the pairs of velocity measurements acquired from the two modalities were found ($\rho = 0.81$), but Bland–Altman analysis indicates a significant bias error. There was relatively weak agreement between the pairs of computed CVR values ($\rho = -0.26$).

Conclusion: Under precise $P_{ET}CO_2$ control, PCMRA proves to be more consistent than TCD. Despite issues with variability, TCD is qualitatively comparable to PCMRA measures of velocity in the MCA. However, PCMRA velocity results are better suited for analyses that require quantitative values, such as CVR.

Key Words: middle cerebral artery; transcranial Doppler; phase contrast; blood flow velocity; cerebrovascular reactivity; CO_2 challenge

J. Magn. Reson. Imaging 2012;00:000–000.

CEREBROVASCULAR REACTIVITY (CVR), defined as a change in cerebral blood flow in response to a vasoactive stimulus, reflects the reserve capacity of the cerebral resistance vessels (1) and can be assessed noninvasively by several imaging modalities including magnetic resonance imaging (MRI). This parameter has shown promise in the assessment of cerebrovascular disease such as carotid artery stenosis and moyamoya (2,3). In practice, CVR imaging relies on the application of a vasoactive stimulus to promote dilation (or constriction) of blood vessels; the reactivity is then inferred by calculating the resultant change in cerebral blood flow. Accurate in vivo quantification of cerebral blood flow, however, is challenging and requires sophisticated imaging strategies such as positron emission tomography or arterial spin labeling. Thus, alternative hemodynamic measures are often substituted in the place of blood flow for CVR calculation. For instance, blood flow velocity (BFV) changes in the middle cerebral artery (MCA) are assumed to reflect overall cerebral blood flow changes within the corresponding cerebral territories (4). This velocity-based method has been demonstrated in various MRI and transcranial Doppler ultrasonography (TCD) studies (5–9).

Phase contrast magnetic resonance angiography (PCMRA) is a tool that is capable of measuring BFV in major cerebral arteries. The MR imaging plane is prescribed perpendicular to a specific artery and bipolar gradients are then applied to induce phase shifts corresponding to the velocity of blood traveling through the plane. PCMRA has undergone extensive validation testing (10,11) and serves as a powerful tool for

[1]Department of Physiology and Experimental Medicine, Hospital for Sick Children, Toronto, Ontario, Canada.

[2]Department of Medical Imaging, University of Toronto, Toronto, Ontario, Canada.

Contract grant sponsor: Canadian Institutes of Health Research.

*Address reprint requests to: A.K., Department of Medical Imaging, University of Toronto, Fitzgerald Building, Rm 127, 150 College Street, Toronto, Ontario, M5S 3E2, Canada.
E-mail: andrea.kassner@utoronto.ca

Received January 11, 2012; Accepted September 25, 2012.

DOI 10.1002/jmri.23911
View this article online at wileyonlinelibrary.com.

ID: selvarajn | Black Lining: [ON] | Time: 13:03 | Path: N:/3b2/JMRI/Vol00000/120359/APPFile/JW-JMRI120359

J_ID: Z3S Customer A_ID: JMRI23911 Cadmus Art: JMRI23911 Ed. Ref. No.: 11-0978.R1 Date: 5-October-12 Stage: Page: 2

verifying the reliability of velocity measurements from other in vivo imaging modalities. However, despite the strengths of MRI, clinical screening for intracranial BFV abnormalities is usually performed using TCD insonation of major cerebral vessels (7,12). TCD is quick, noninvasive, and its high temporal resolution is well suited for studying dynamic cerebrovascular responses. However, TCD also suffers from measurement variability, as velocity readings are strongly dependent on operator skill, the availability of an ultrasonic window in the skull, and the ability to detect distal branches of intracranial vessels (7). In addition, the insonation angle stemming from the misalignment of the ultrasound beam with the direction of blood flow can produce significant measurement errors if not properly accounted for.

To date, only a handful of verification studies exist between TCD and PCMRA velocity measurements in the MCA (13,14), with even fewer involving CVR (6,15). There is currently no strong consensus within these studies regarding the agreement between the two modalities, possibly due to a lack of systematic control over spontaneous changes in subject carbon dioxide (CO_2) and oxygen (O_2) levels (8), which have known vasoactive properties. Recently, a computer-controlled model-driven prospective end-tidal targeting (MPET) system has been introduced that enables accurate manipulation of subject CO_2 and O_2 by precisely regulating the composition of gas delivered to the subject. This method of controlled respiratory challenge is quantified by noninvasive monitoring of the end-tidal partial pressures of the subject's expired O_2 ($P_{ET}O_2$) and CO_2 ($P_{ET}CO_2$) (16) and has been shown to improve reproducibility of CVR data (17).

This study compared the measurements of middle cerebral artery BFV and CVR obtained with TCD and PCMRA while making use of the MPET system in order to control the confounding physiological variations associated with CO_2 stimulation. We hypothesized that PCMRA and TCD velocity will be correlated, but TCD data will have higher measurement variability. We further proposed a TCD angle correction strategy and assessed whether it could remove the angle dependence of TCD results, therefore possibly improving the comparison between the two techniques.

MATERIALS AND METHODS

Subject Recruitment

Nine healthy, nonsmoking, male volunteers (21–31 years) with no history of respiratory, cardiovascular, or cerebrovascular disease were recruited for this study. All procedures were approved by our Institutional Review Board, and informed written consent was obtained from each subject. Consumption of vasoactive substances such as caffeine or alcohol was prohibited on the day of imaging.

Delivery of Vasoactive Stimulus

Changes in $P_{ET}CO_2$ were achieved by introducing controlled amounts of the CO_2 stimulus combined with a steady supply of medical air through a rebreathing circuit and mask. These masks were fitted onto the subjects and connected to the MPET system (RespirAct; Thornhill Research, Toronto, Canada). The MPET regulates the flow and composition of the gas stimulus delivered while simultaneously ensuring adequate oxygen supply to the subject for accurate targeting of $P_{ET}CO_2$ and $P_{ET}O_2$, which have been shown to closely correlate with arterial blood gas values (18). A detailed description of the MPET system is provided by Slessarev et al (16).

In this study, baseline and hypercapnia states were defined as the periods when subject $P_{ET}CO_2$ was targeted at 40 mmHg and 45 mmHg, respectively; $P_{ET}O_2$ was maintained at 100 mmHg. Partial pressures of exhaled gas were continuously monitored via sampling lines connected to the mask and end-tidal values were recorded at the end of each expired breath to define the measured $P_{ET}CO_2$ and $P_{ET}O_2$ waveforms.

All subjects were given an orientation before imaging to become familiar with the experiment and the MPET system. Next, subjects underwent CVR imaging, first with TCD, followed by PCMRA.

TCD-Based CVR Imaging

TCD evaluation was conducted using a commercial duplex ultrasound system (iU22 xMatrix; Philips Electronics, Best, Netherlands) with a 2.0 MHz transducer operated by an experienced sonographer (A.M.). With subjects in the supine position, the M1 segment of right MCA was identified via insonation of the transtemporal window. Upon isolating the site of highest flow velocity within the segment, the position of the transducer was held constant for subsequent measurements. The baseline state was then targeted using the MPET system, after which multiple TCD velocity waveforms recordings were acquired and saved on the ultrasound console for analysis. As per standard TCD protocol, the insonation angle was not considered in the measurement. End-tidal levels were maintained steady for the duration of the assessment, which was ~2 minutes. Without moving the ultrasound transducer, the measurement was performed again during targeted hypercapnia. Once both measurements were completed, the location of the transtemporal window as well as the insonation depth were recorded for the purpose of spatial colocalization on the MR images. This process was repeated for the left MCA.

PCMRA-Based CVR Imaging

Following TCD assessment, the subjects were imaged on a 3.0T clinical MRI (MAGNETOM Tim Trio; Siemens Medical Solutions, Erlangen, Germany). The transtemporal windows on each subject's head was marked with glycerol-water capsules, as defined by the locations recorded during TCD evaluation. A standard 3D time-of-flight (TOF) sequence was run to identify the left and right MCAs as well as the capsule positions to guide PCMRA slice positioning.

Imaging planes for PCMRA scans were prescribed to measure, as closely as possible, the same location as

ID: selvarajn | Black Lining: [ON] | Time: 13:03 | Path: N:/3b2/JMRI/Vol00000/120359/APPFile/JW-JMRI120359

COLOR

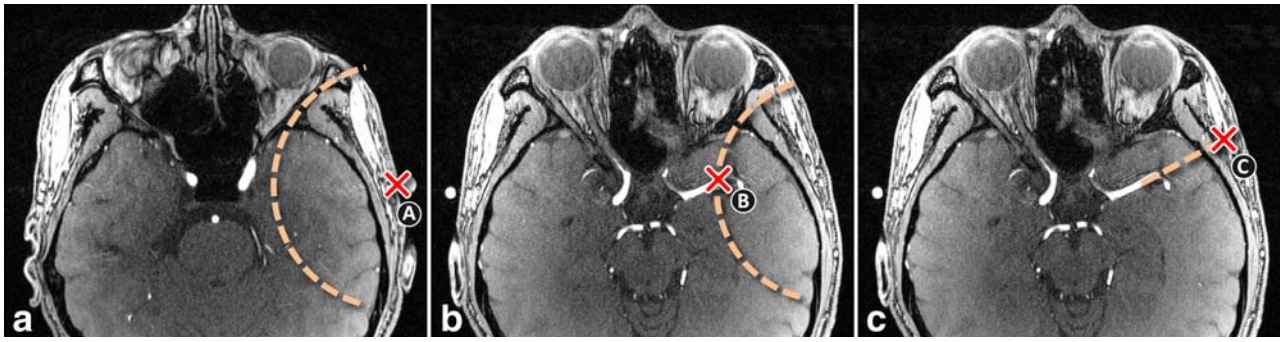

Figure 1. Determining the insonation angle by identifying three points (marked by an ×) on the 3D-TOF images. A radial projection of length equal to the insonation depth is projected from the glycerol-water capsule in (**a**) and intersects the MCA in a distant slice in (**b**). Direction of blood flow is characterized in (**c**).

acquired by TCD. For each MCA, the site of TCD velocity measurement was approximated on the 3D-TOF image by projecting a straight line from the capsule marker to the vessel with length equal to the recorded insonation depth. A single slice was then prescribed with double-oblique angle to the blood flow direction. Similar to the TCD protocol, PCMRA images were acquired during sustained baseline and hypercapnia states controlled by the MPET system for both the left and right MCA. The imaging parameters for the PCMRA sequence were as follows: repetition time (TR) = 52.75 msec, echo time (TE) = 5.17 msec, flip angle (FA) = 30°, matrix = 364 × 448, voxel size = 0.4 × 0.4 × 5.0 mm, bandwidth = 399 Hz/pixel, velocity encoding (V_{enc}) = 75 cm/s, acquisition time ~3.5 minutes. Retrospective gating from a pulse oximeter was applied and a total of 20 phases per cardiac cycle were acquired.

Data Analysis

TCD waveform measurements were automatically converted to time-averaged peak velocities (TAPV) by the ultrasound system. This parameter was calculated from the mean value of the velocity envelope for a single cardiac cycle in each waveform. Only the highest TAPV within each set of multiple measurements were saved.

A correction factor derived from the insonation angle was also applied to compensate for the underestimation of TCD velocities in the MCA caused by misalignment of the Doppler signal to the direction of blood flow. This angle was determined for each measurement by identifying the coordinates of three spatial landmarks on the 3D-TOF volume, as illustrated in Fig. 1. The first point (point A), marked by the glycerol-water capsule, represents the position of the ultrasound transducer during TCD insonation. Next, a spherical projection with radius equal to the insonation depth was extended from the capsule to determine its intersection with the MCA (point B), which corresponds to the site of TCD velocity assessment. A third point (point C) is placed along the line formed by the tangent to the MCA at point B. These three points define two line segments: AB giving the path of insonation and BC giving the expected direction of blood flow at the site of insonation. The angle (θ) between these two lines was used for TCD angle correction, as represented by the following relation:

$$\mathrm{TCD}_{\mathrm{corr}} = \frac{\mathrm{TCD}}{\cos\theta} \quad [1]$$

MRI data were transferred to an independent workstation for analysis with MatLab (MathWorks, Natick, MA) using in-house scripts. Phase images were first corrected for phase wrapping, and then quantified into velocity values derived from the V_{enc}. The temporal mean velocity for each voxel was calculated by averaging over the 20 cardiac phases. A representative TAPV for each PCMRA image was assigned from the voxel with highest mean velocity within the MCA.

Velocity-based CVR for both TCD and PCMRA was determined for each pair of baseline/hypercapnia BFV measurements. This value was expressed as the change in TAPV between baseline and hypercapnia, divided by the change in $P_{ET}CO_2$ (5 mmHg). In addition, the reactivity was normalized to a percent change (%CVR) relative to the baseline TAPV:

$$\%\mathrm{CVR} = \frac{\mathrm{TAPV}_{\mathrm{HYP}} - \mathrm{TAPV}_{\mathrm{BL}}}{\Delta \mathrm{CO}_2} \times \frac{1}{\mathrm{TAPV}_{\mathrm{BL}}} \times 100\% \quad [2]$$

The correlation between the two modalities was assessed using a nonparametric test (Spearman's rho) and their relation was visualized on a Bland–Altman plot. The mean and coefficient of variation (%CV) within each type of measurement were also calculated.

RESULTS

All nine subjects were fully compliant with the protocol, and velocity data from 17 out of 18 MCAs were acquired in total. One MCA measurement could not be completed due to technical difficulties.

Sampled end-tidal values confirmed accurate targeting of $P_{ET}CO_2$ and $P_{ET}O_2$ during the application of the MPET system for both TCD and PCMRA imaging. Average baseline and hypercapnia state $P_{ET}CO_2$ were 40.2 ± 0.8 mmHg and 45.1 ± 0.5 mmHg, respectively. $P_{ET}O_2$ averaged 103.2 ± 3.1 mmHg during

Table 1
Average and %CV of Measured Velocity and %CVR

	Baseline TAPV		Hypercapnia TAPV		%CVR	
	cm/s	%CV	cm/s	%CV	%/mmHg	%CV
PCMRA	58.2	16.2%	69.9	15.7%	3.9	30.6%
TCD	64.6	28.4%	77.2	25.2%	4.2	54.8%
Angle corrected TCD	76.1	32.3%	91.8	27.9%	—	

TAPV, time-averaged peak velocity; %CVR, normalized cerebrovascular reactivity; %CV, coefficient of variation.

baseline imaging and 106.7 ± 2.5 mmHg during hypercapnia, closely matching the study targets.

TAPV measurements in the MCA and corresponding %CVR values are summarized in Table 1. In general, PCMRA yielded lower BFV for both baseline and hypercapnia, but was also the most consistent with a significantly lower %CV compared to Doppler measurements. Slightly higher average velocities were observed using TCD, and application of angle correction (mean angle = 29.7 ± 15.0°) significantly widened the difference. For CVR, mean TCD and PCMRA measures were comparable, but the variability of the PCMRA method was markedly lower than TCD.

Spearman's rank analysis showed a strong correlation between the TCD and PCMRA ($\rho = 0.81$) that was negatively impacted after angle correction ($\rho = 0.68$), as presented in Fig. 2. In the Bland–Altman plots of Fig. 3, a proportional bias error is apparent in both the uncorrected and angle-corrected TCD comparison with PCMRA, as the discrepancies are positively skewed with increasing BFV. Figure 4a,b presents the Spearman's rank correlation and Bland–Altman analysis between %CVR values obtained from the two methods. Very poor correlation ($\rho = -0.26$) as well as a significant error range and proportional bias was observed in the comparison.

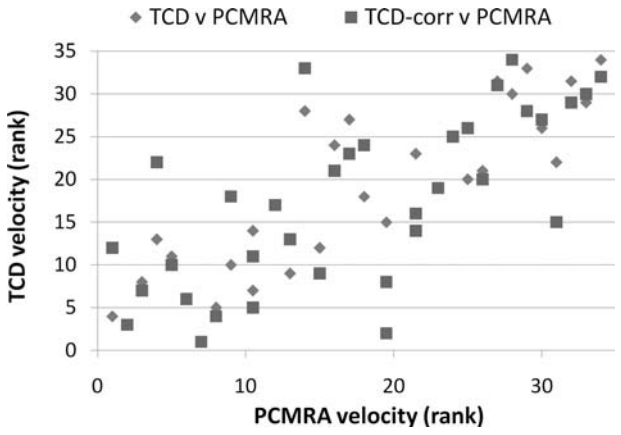

Figure 2. Spearman's rho analysis of TAPV obtained by PCMRA versus TCD (◆) and angle corrected TCD (■). The correlation coefficients are $\rho = 0.81$ and $\rho = 0.68$, respectively.

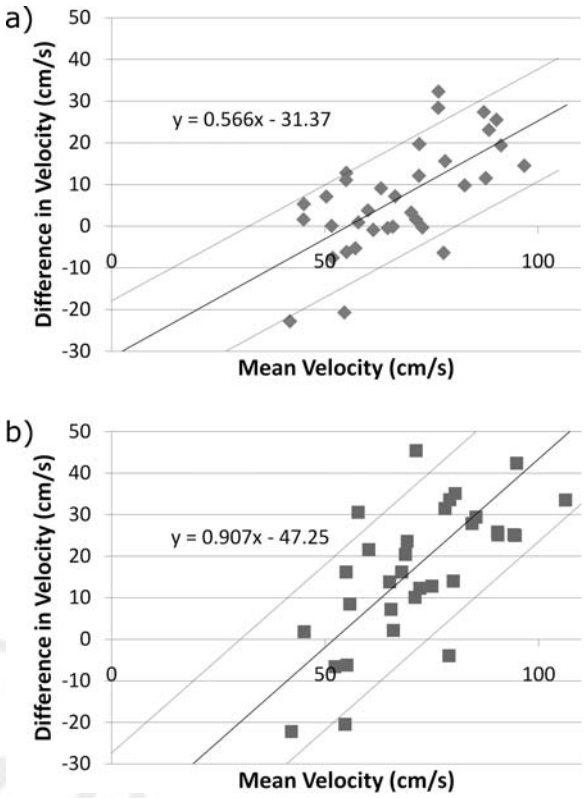

Figure 3. Bland–Altman plot of mean versus difference between velocities measured by PCMRA and TCD (**a**) before angle correction with 95% confidence interval of ±13.5 cm/s, and (**b**) after angle correction with confidence interval of ±19.9 cm/s. The equation signifying a positive trend in the bias is displayed in each plot.

DISCUSSION

This study provides a comparison between TCD and PCMRA measurements of velocity as well as velocity changes induced by hypercapnia. In contrast to prior studies, an MPET system was used to minimize variability of subject $P_{ET}CO_2$ and $P_{ET}O_2$. This additional control of the stimulus ensured that the results accurately reflect the merits of each modality by minimizing confounding effects.

First-order analysis of TAPV measurements showed good correlation between the two methods, despite TCD exhibiting higher average values and greater %CVs. These findings are in line with results published in previous studies of the MCA. Baledent et al (13) noted a consistent overestimation of peak-systolic and end-diastolic velocities by TCD compared to PCMRA, even though the two methods exhibited moderate correlation. Likewise, Seitz et al (14) found TCD produced higher velocities in the MCA. The discrepancy is explained, in part, by a well-known spectral broadening effect in TCD measurements, which can lead to artificial increases in received spectral frequencies at higher insonation angles (19). Furthermore, the limited spatial resolution of PCMRA may lead to partial volume effects and reduce the peak velocity measurement, especially in smaller vessels where the parabolic velocity profile will have a much

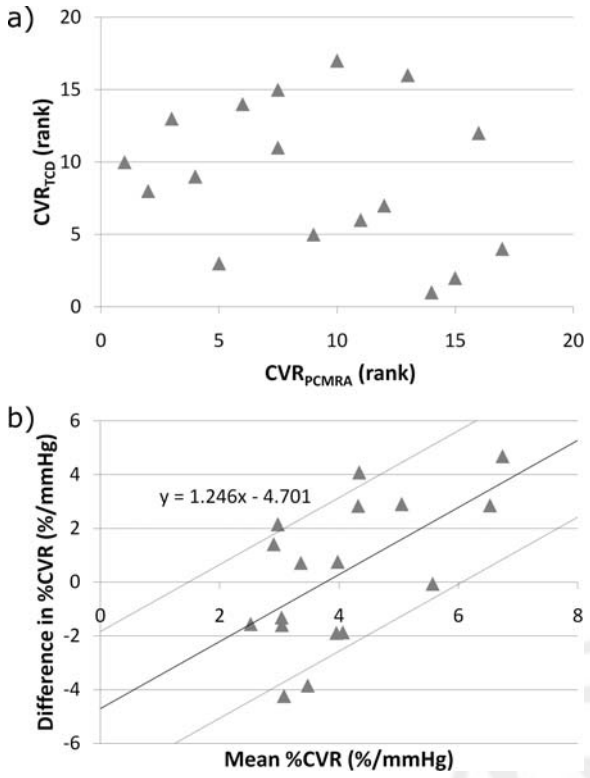

Figure 4. **a**: Spearman's rho analysis of %CVR values calculated from PCMRA versus TCD ($\rho = -0.26$). **b:** Bland–Altman plot of mean versus difference between %CVR calculated from PCMRA and TCD velocities (95% confidence interval ±2.86%).

steeper gradient (11,20). A possible approach for circumventing these issues is to compare mean velocity through the vessel. Partial voluming in PCMRA will naturally reduce with the larger area, while spurious peaks from TCD may be mitigated by measuring intensity-weighted mean of the signal (21). However, the comparison between mean velocity was not explored in this study, as the focus was on TAPV.

The Bland–Altman plots of the velocity and CVR data pairs show a linearly proportional bias indicating an increasing offset error for higher BFV. Although partial volume effects in MRI do become more pronounced when the parabolic flow profile becomes less blunted as velocity increases, it does not explain the magnitude of the observed bias. Our data indicate that the relation between TCD and PCMRA inherently does not follow a unit slope, resulting in significant measurement differences during hypercapnia. Conversely, MCA velocities measured during baseline happen to occur in the region where the error is lowest (50–70 cm/s), as shown in Fig. 3a. Without the stimulus in our study, the discrepancy between these two modalities would not be very evident. The proportional error carries over to the CVR calculations as TCD exhibits a greater change in velocities between baseline and hypercapnia compared to PCMRA, thus explaining the positive slope in Fig. 4b. It is worth noting that the limits of agreement in the Bland–Altman plots remain fairly consistent, suggesting that a simple conversion factor is possible between TCD and PCMRA velocities. However, the effect of various parameters such as vessel size and MRI spatial resolution need to be better understood before such techniques are proposed.

Angle correction of TCD data widened the velocity difference between the two methods and also reduced their statistical dependence. The choice to use capsule markers to calculate the angles was based on the inherent difficulty in obtaining an accurate estimate of the insonation angle from the ultrasound color image (22). The angles calculated in our study are in concordance with literature on TCD assessment of the MCA (22), ruling out improper placement of the capsules as a significant source of error. Previously, Seitz et al (14) implemented a similar method for estimating the insonation angle using the intensity projection of an MRA. Their angle correction of MCA velocities also resulted in higher variability and poor correlation with MRI. The 3D method in our study was proposed to overcome the limitations of deriving angles from a projection. Based on the similar outcomes, it appears that other sources of error such as the aforementioned spectral broadening may have a cumulative impact that is not accounted for by angle correction. Also, validity of the angle factor may be significantly compromised if the assumption of laminar flow in the MCA does not hold true. In the presence of turbulent or skewed flow, TCD may be measuring the velocity of scatterers that are not flowing in the same orientation as the vessel. Our introduction of a robust angle correction scheme was unable to improve TCD correlation and, therefore, a thorough examination of the effectiveness of angle correction should be performed in future studies.

Despite a large number of studies asserting the value of TCD-CVR (8,9), studies comparing velocity-based CVR in smaller vessels are rare. The most recent publication assessed the reactivity from hyperventilation and found very weak correlation between TCD and PCMRA (15). Our study has demonstrated a similar trend, where good correlation between velocity measurements does not translate into correlation among the corresponding %CVR values. In terms of variability, the %CVs of the PCMRA-CVR values are again significantly lower than TCD-CVR, even though the average values are very similar. This may suggest an issue beyond operator dependence, as the transducer position is fixed between baseline and hypercapnia measurements. One distinction between the TCD and PCMRA methods is their temporal base, with PCMRA forming an average velocity profile over a period of several minutes, while the TCD waveform was sampled here over a single cardiac cycle. Fluctuations in blood flow on time scales between these limits would contribute to variability in the TCD measurements, but be largely averaged out of the PCMRA results. Such factors were not taken into account in our study and require further investigation.

In conclusion, we have demonstrated a disconnect between TCD and MRI measures of BFV in the MCA that needs to be addressed. TCD is a widely accepted tool in clinical practice, in large part due to its accessibility and relatively low cost. However, as more

J_ID: Z3S Customer A_ID: JMRI23911 Cadmus Art: JMRI23911 Ed. Ref. No.: 11-0978.R1 Date: 5-October-12 Stage: Page: 6

sophisticated assessment methods requiring quantitative measures (such as CVR) are developed, it is important to rigorously validate the accuracy and reliability of TCD against other established modalities.

ACKNOWLEDGMENTS

We thank our MR technologists Tammy Rayner, Ruth Weiss, Garry Detzler, and Annette Weekes for operating the MR scanner, Olivia Pucci and colleagues at Thornhill Research Inc. for technical support on the RespirAct, and George Tomlinson for helpful discussion on the statistical analysis. We also thank all the participants who volunteered their time for this study.

REFERENCES

1. Yonas H, Pindzola RR. Physiological determination of cerebrovascular reserves and its use in clinical management. Cerebrovasc Brain Metab Rev 1994;6:325–340.
2. Markus H, Cullinane M. Severely impaired cerebrovascular reactivity predicts stroke and TIA risk in patients with carotid artery stenosis and occlusion. Brain 2001;124:457–467.
3. Mikulis DJ, Krolczyk G, Desal H, et al. Preoperative and postoperative mapping of cerebrovascular reactivity in moyamoya disease by using blood oxygen level-dependent magnetic resonance imaging. J Neurosurg 2005;103:347–355.
4. Rijbroek A, Boellaard R, Vriens EM, Lammertsma AA, Rauwerda JA. Comparison of transcranial Doppler ultrasonography and positron emission tomography using a three-dimensional template of the middle cerebral artery. Neurol Res 2009;31:52–59.
5. Kario K, Ishikawa J, Hoshide S, et al. Diabetic brain damage in hypertension: role of renin-angiotensin system. Hypertension 2005;45:887–893.
6. Patrick JT, Fritz JV, Adamo JM, Dandonna P. Phase-contrast magnetic resonance angiography for the determination of cerebrovascular reserve. J Neuroimaging 1996;6:137–143.
7. Markus HS. Transcranial Doppler ultrasound. Br Med Bull 2000; 56:378–388.
8. Aries MJ, Elting JW, De Keyser J, Kremer BP, Vroomen PC. Cerebral autoregulation in stroke: a review of transcranial Doppler studies. Stroke 2010;41:2697–2704.
9. Panerai RB. Transcranial Doppler for evaluation of cerebral autoregulation. Clin Auton Res 2009;19:197–211.
10. Spilt A, Box FM, van der Geest RJ, et al. Reproducibility of total cerebral blood flow measurements using phase contrast magnetic resonance imaging. J Magn Reson Imaging 2002;16:1–5.
11. Machida H, Komori Y, Ueno E, et al. Spatial factors for quantifying constant flow velocity in a small tube phantom: comparison of phase-contrast cine-magnetic resonance imaging and the intraluminal Doppler guidewire method. Jpn J Radiol 2009;27: 335–341.
12. Aaslid R, Markwalder TM, Nornes H. Noninvasive transcranial Doppler ultrasound recording of flow velocity in basal cerebral arteries. J Neurosurg 1982;57:769–774.
13. Baledent O, Fin L, Khuoy L, et al. Brain hydrodynamics study by phase-contrast magnetic resonance imaging and transcranial color doppler. J Magn Reson Imaging 2006;24:995–1004.
14. Seitz J, Strotzer M, Schlaier J, Nitz WR, Volk M, Feuerbach S. Comparison between magnetic resonance phase contrast imaging and transcranial Doppler ultrasound with regard to blood flow velocity in intracranial arteries: work in progress. J Neuroimaging 2001;11:121–128.
15. Valdueza JM, Balzer JO, Villringer A, Vogl TJ, Kutter R, Einhaupl KM. Changes in blood flow velocity and diameter of the middle cerebral artery during hyperventilation: assessment with MR and transcranial Doppler sonography. AJNR Am J Neuroradiol 1997; 18:1929–1934.
16. Slessarev M, Han J, Mardimae A, et al. Prospective targeting and control of end-tidal CO2 and O2 concentrations. J Physiol 2007; 581:1207–1219.
17. Kassner A, Winter JD, Poublanc J, Mikulis DJ, Crawley AP. Blood-oxygen level dependent MRI measures of cerebrovascular reactivity using a controlled respiratory challenge: reproducibility and gender differences. J Magn Reson Imaging 2010;31:298–304.
18. Ito S, Mardimae A, Han J, et al. Non-invasive prospective targeting of arterial P(CO2) in subjects at rest. J Physiol 2008;586: 3675–3682.
19. Hoskins PR. Accuracy of maximum velocity estimates made using Doppler ultrasound systems. Br J Radiol 1996;69:172–177.
20. Hoogeveen RM, Bakker CJ, Viergever MA. MR phase-contrast flow measurement with limited spatial resolution in small vessels: value of model-based image analysis. Magn Reson Med 1999;41: 520–528.
21. Poulin MJ, Robbins PA. Indexes of flow and cross-sectional area of the middle cerebral artery using Doppler ultrasound during hypoxia and hypercapnia in humans. Stroke 1996;27: 2244–2250.
22. Krejza J, Mariak Z, Babikian VL. Importance of angle correction in the measurement of blood flow velocity with transcranial Doppler sonography. AJNR Am J Neuroradiol 2001;22: 1743–1747.